Climate variability and density-dependent population dynamics: Lessons from a simple High Arctic ecosystem

Dominique Fauteux[a,1], Audun Stien[b], Nigel G. Yoccoz[b], Eva Fuglei[c], and Rolf A. Ims[b]

[a]Canadian Museum of Nature, Centre for Arctic Knowledge and Exploration, Gatineau, QC, Canada, J9J 3N7; [b]Department of Arctic and Marine Biology, University of Tromsø–The Arctic University of Norway, N-9037 Tromsø, Norway; and [c]Norwegian Polar Institute, N-9296 Tromsø, Norway

Ecologists are still puzzled by the diverse population dynamics of herbivorous small mammals that range from high-amplitude, multiannual cycles to stable dynamics. Theory predicts that this diversity results from combinations of climatic seasonality, weather stochasticity, and density-dependent food web interactions. The almost ubiquitous 3- to 5-y cycles in boreal and arctic climates may theoretically result from bottom-up (plant–herbivore) and top-down (predator–prey) interactions. Assessing, empirically, the roles of such interactions and how they are influenced by environmental stochasticity has been hampered by food web complexity. Here, we take advantage of a uniquely simple High Arctic food web, which allowed us to analyze the dynamics of a graminivorous vole population not subjected to top-down regulation. This population exhibited high-amplitude, noncyclic fluctuations—partly driven by weather stochasticity. However, the predominant driver of the dynamics was overcompensatory density dependence in winter that caused the population to frequently crash. Model simulations showed that the seasonal pattern of density dependence would yield regular 2-y cycles in the absence of stochasticity. While such short cycles have not yet been observed in mammals, they are theoretically plausible if graminivorous vole populations are deterministically bottom-up regulated. When incorporating weather stochasticity in the model simulations, cyclicity became disrupted and the amplitude was increased—akin to the observed dynamics. Our findings contrast with the 3- to 5-y population cycles that are typical of graminivorous small mammals in more complex food webs, suggesting that top-down regulation is normally an important component of such dynamics.

population fluctuations | tundra ecosystem | trophic interactions | seasonality | bottom-up regulation

Theory suggests that contrasting population dynamics result from details in the pattern of density dependence, including its strength, whether it acts instantly or with a delay, and how it interacts with deterministic (seasonal) and stochastic (weather) components of the prevailing or changing climate (1–5). Studies of small rodents have contributed much to elucidating the different facets of density-dependent and density-independent population dynamics (2, 4). A central topic has been what sort of density dependence yields the high-amplitude, multiannual population cycles for which voles and lemmings have become so renowned (6–9). Based on time series analyses, delayed density dependence is considered to be a main determinant of population cycles (see refs. 4, 10 for reviews), although overcompensatory direct density dependence appears to be an alternative in some settings (11). As rodent cycles are most prevalent in northern ecosystems with profound climatic seasonality (refs. 6, 7, 12, but see refs. 13, 14), several studies have emphasized that annual density dependence ought to be decomposed into its seasonal components (15–17)—both to accurately account for the density-dependent structure that underlies the observed dynamics and to identify the season-specific biotic mechanisms that cause density dependence. Considering seasonal dynamics is also crucial to assessing the role of climatic change and weather stochasticity because both differ between summer and winter (15, 18). The role of climate forcing is now

also emphasized by the recent collapses and dampening of population cycles in several ecosystems that appear to be associated with ongoing climate change (15, 19, 20).

Linking density dependence to the biotic mechanisms that causally generate the diversity of population dynamics patterns seen in small mammals has proved to be challenging. Most rodent populations are imbedded in complex food webs and, hence, simultaneously subjected to a multitude of biotic interactions that could cause the different facets of density-dependent population growth. For instance, density dependence may result from both top-down and bottom-up trophic interactions as well as intrinsic population mechanisms (11, 21, 22). While field experiments have helped pinpoint some mechanisms (23–27), they have been too short term to be conclusive with respect to what generates different patterns of multiannual population dynamics.

Here, we apply an approach that has proved useful for unraveling the effects of density dependence and weather stochasticity in herbivorous large mammals (e.g., refs. 28–30), namely to target populations that are found in exceptionally simple biotic settings. Hence, our study targets a High Arctic population of the graminivorous (grass-eating) East European vole (*Microtus levis*) in a food web that lacks significant top-down regulation (i.e., predation). By combining statistical analyses of long-term, high-quality live-trapping data with simulations of a population model parameterized from these data, we 1) estimate the seasonal density dependence and resultant population dynamics (e.g., cyclic or noncyclic) that emerge in such a simple biotic setting and 2) assess how climatic

Significance

Whether the renowned population cycles of small mammals in northern food webs are driven by bottom-up (plant–herbivore) or top-down (predator–prey) interactions is still a debated question but crucial to our understanding of their ecological functions and response to climate change. A long-term study of a graminivorous vole population in an exceptionally simple High Arctic food web allowed us to identify which population dynamics features are present without top-down regulation. Unique features were high-amplitude, noncyclic population fluctuations driven by a combination of stochastic weather events and season-specific density dependence likely arising from plant–herbivore interactions. That such features are not present in more complex food webs points to the importance of top-down regulation in small mammal populations.

ECOLOGY

seasonality and weather stochasticity in terms of rain-on-snow (ROS) events in winter impinge on such density-dependent population dynamics. Finally, we point out how the insights from this unique case study shed light on the longstanding puzzle about what generates population cycles and how ongoing climate change may influence these cycles.

Results

Annual Population Dynamics. The 1991 to 2007 time series of Eastern European vole densities from the Ridge trapping area was characterized by high-amplitude population fluctuations with 2 to 4 y between subsequent crash years (Fig. 1). The population dynamics appeared to be stationary (i.e., there was no evidence for temporal trends in mean or variance in densities over the 18 y). The amplitude of the fluctuations (s-index = 0.57) was within the range found in population time series of cyclic Arctic lemming populations (31). However, in contrast to most other Arctic populations, first- ($r = -0.39$) and second-order ($r = 0.02$) autocorrelation coefficients showed no evidence of cyclic dynamics.

Seasonal Density Dependence. Population densities in the Core trapping area showed the same annual pattern as densities in the Ridge area (cross-correlation of vole densities with the Ridge trapping area, $r = 0.92$; Fig. 1). Within the summer season, monthly population growth rates were all positive (Figs. 2 and 3A). This suggests that vole population densities remained below carrying capacity in summer. Still, there was evidence for negative density dependence in the monthly population growth rates (Table 1 and Fig. 3A). Detailed demographic analyses suggested that the density dependence in population growth in summer was partly due to density-dependent survival in both sexes (*SI Appendix*, Table S2 and Fig. S2) and strong density-dependent regulation of adult male densities (*SI Appendix*, Fig. S2).

In contrast, winter monthly population growth rates were negative in many of the years. This difference between seasons was due to maximum population growth rate in winter (at low population densities and ROS) being one-third the maximum population growth rate in summer (β_0 in Table 1), while the effect size of density was similar in the two seasons (β_D in Table 1). In addition, negative population growth rates in winter were associated with high levels of ROS in the winter (Table 1 and Fig. 3B). Overall, the data suggest that density dependence in winter led to strong overcompensatory population regulation (i.e., negative realized growth).

Simulated Population Dynamics. Simulation of the deterministic version of the seasonal density-dependent model (Eqs. **2**, **5**, and **6**) generated stable 2-y vole cycles. These 2-y cycles were relatively robust to changes in climate severity in winter, in that high ROS must become the norm before we expect a change to stable dynamics with a single equilibrium density (Fig. 4A). The 2-y cycle in the baseline model was also robust to changes in season lengths as climate change would have to reduce the winter length to well below 8 mo for more complex dynamics to appear (Fig. 4B). However, the signal of the 2-y cycles deteriorated rapidly with increasing levels of stochastic process error (Fig. 4C). At the observed levels of process error, as generated by stochastic variation in winter ROS, the expected second-order autocorrelation was close to zero in the model simulations ($r = 0.02$) (i.e., similar to what was estimated from the time series data). Finally, temporal variability as quantified by the s-index increased with increasing process error (Fig. 4D).

Discussion

Without significant top-down regulation from predators or interspecific competition, the focal study system is essentially reduced to a simple two-link food chain consisting of a multivoltine herbivore population and their graminoid food plants in a profoundly seasonal environment. Here, we have presented an empirical analysis of such an ecological system that previously has been subjected to only theoretical investigations. Such systems have been modeled mechanistically in continuous time to identify under which circumstances multiannual herbivore population cycles can be expected (32, 33). Moreover, theoreticians have thoroughly investigated the dynamical properties of phenomenological discrete-time models with seasonal density dependence (34), akin to the model we parameterized here with field data. The core insight from this theory—and indeed also our empirical study—is that the profound seasonality destabilizes the dynamics of such simple systems (35). Profound seasonality in terms of a long Arctic winter without primary production implies that the carrying capacity in summer greatly exceeds that of the winter. Such an environmental setting combined with a multivoltine life history and rapid population growth in summer allows the herbivore population to overshoot its winter carrying capacity. We provide evidence that such a situation prevails in the graminivorous East European voles on Svalbard. While density dependence frequently causes population crashes over winter, the population does not reach the higher densities needed for negative population growth to occur over summer.
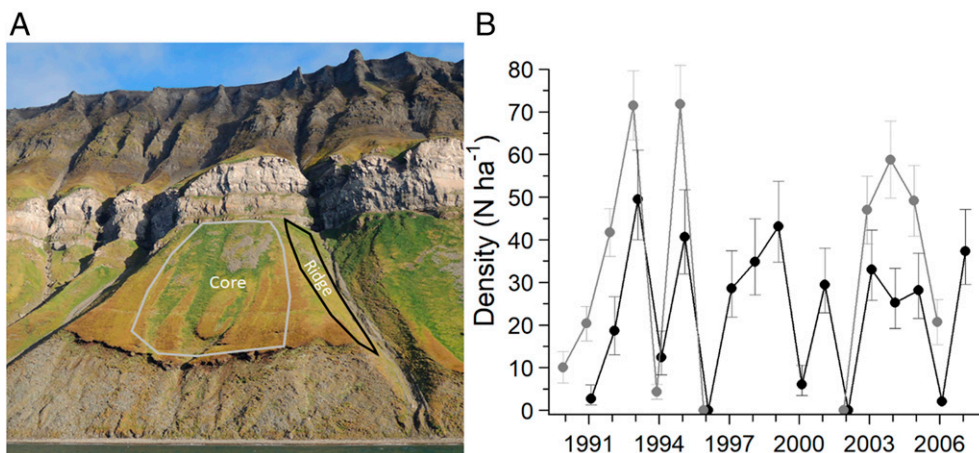

Fig. 1. Picture of the Core and Ridge areas for live trapping East European voles near Grumantbyen on Svalbard (*A*) and time series of vole densities (*B*) estimated in August in the Core area (gray shape, lines, and points; years 1990 to 1996 and 2002 to 2006) and the Ridge area (black shape, lines, and points; years 1991 to 2007). Error bars represent 95% CIs.
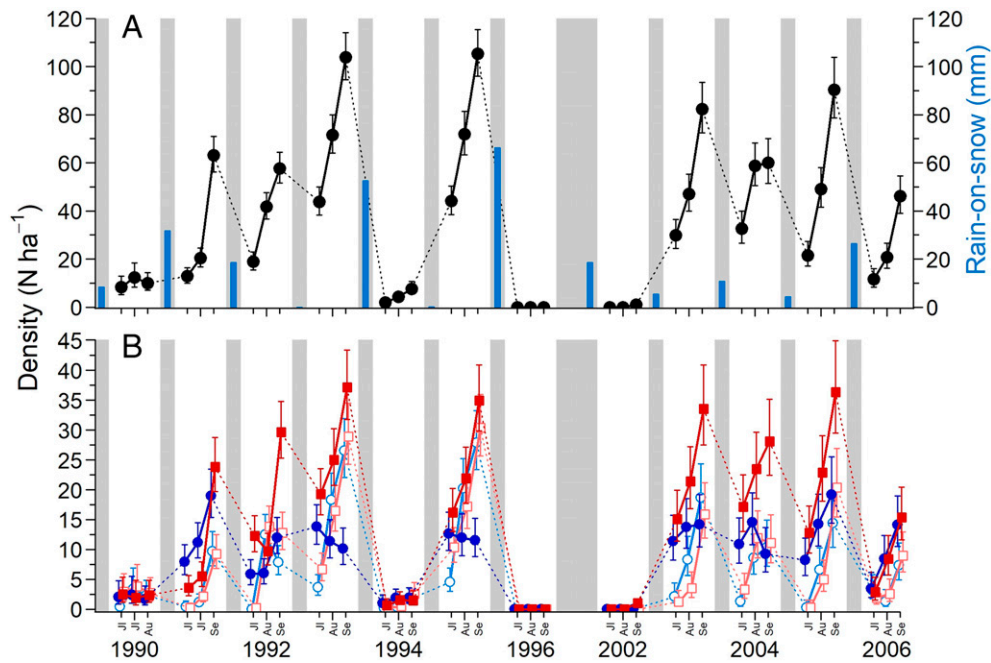
Fig. 2. Population density of the East European vole in the Core area near the Grumant area in Svalbard (lines and points) and precipitation as ROS during the previous winter (blue bars in *A* only). The total population densities are shown in *A*. In *B*, adult males (solid blue circles and lines), adult females (solid red squares and lines), subadult males (open pale blue circles and lines), and subadult females (open pale red squares and lines) are shown. Densities were obtained using spatially explicit capture–recapture models with the Huggins parameterization. Dotted lines indicate change in population size during winter. The thin gray bands indicate winter when trapping was not conducted. The wide gray band between 1996 and 2002 indicates no trapping during that period. Error bars represent 95% CIs. Notice the difference in scale between *A* and *B*. In 1990, trapping periods were in early July, late July, and mid-August. In 1991, trapping periods were early July, late July, and mid-September, whereas for all other years, trapping was done in the first part of each month.

It is well known that discrete-time models with seasonal density dependence, like our baseline model, can generate 2-y cycles (34). Interestingly, the continuous-time, plant–herbivore model analyzed by Turchin and Batzli (33)—with a graminoid-type plant regrowth function, multivoltine herbivore population dynamics, and High Arctic seasonality without stochasticity—also generates 2-y cycles, even though the seasonal dynamics is very different from what is seen in the discrete-time models and our empirical data (*SI Appendix*). This emphasizes the general propensity of seasonality to generate 2-y cycles in this system. Still, we are not aware that such short population cycles have ever been reported for any mammal population. Neither are we aware of any other examples of the noncyclic high-amplitude, high-frequency boom–bust vole population dynamics we observed in our High Arctic study system. In multivoltine rodents, cycle lengths typically vary between 3 and 5 y in ecosystems with profound seasonality, while populations in environments with less pronounced seasonality have typically noncyclic, low-amplitude fluctuations that often are categorized as stable dynamics (36, 37). It is commonly assumed that cycle-generating mechanisms have delayed effects on population density, such as extended periods of food depletion or predation over more than one phase (4, 10, 12, 21), while opinions differ about which mechanisms are in place (38, 39). Seasonality is in itself a source of delay in producer–consumer interactions (32) but is expected to yield, at most, 2-y cycles. Also, the rapid regrowth of graminoids (33)—even after high vole peak densities and severe winter grazing (40)—prevents longer delays that may generate the longer cycles often found in graminivorous voles. Our results also imply that delayed intrinsic mechanisms, such as stress-induced maternal effects (41), were not present. Finally, our study is consistent with the hypothesis that the almost ubiquitous guild of specialist rodent predators in boreal and Arctic food webs normally cause the delays in density dependence that generate the longer vole cycles in that the predator guild was lacking in our

study system (39, 42, 43). Indeed, the unique absence of top-down regulation by specialist predators in High Arctic Svalbard is the most likely cause of the exceptional vole population dynamics observed. Experimental predator removals (24, 27, 40) have never been conducted at a sufficient spatial and temporal scale to investigate whether a similar outcome would appear in other vole populations released from top-down regulation.

A fundamental question in population ecology accentuated by global climate change is how abiotic environmental variation can modify the effect of density-dependent biotic interactions. Our study adds to previous studies showing that episodes of mild winter weather in boreal and Arctic ecosystems, through increased ROS events and changes in snow conditions, may lead to population crashes in herbivores (44–46) and disrupt population cycles (18–20, 47). Previous models have shown that climatically disrupted population cycles in multivoltine rodents readily collapse to low-amplitude fluctuations and, hence, stable population dynamics (19, 20, 47). Here, we have shown that population cycles in a very simple trophic system may also be disrupted by increasing weather stochasticity but without any dampening effect on the dynamics. Hence, our case study provides support to the general conjecture that the impact of climate change on ecological systems depends on their structure and hence can be expected to be diverse across time and space (18, 19, 29).

Materials and Methods

Study Population. Our study was located at Grumant in Svalbard (78.18°N, 15.13°E). This High Arctic location is characterized by cool summers (July average: 5.9 °C) and cold winters (January average: −16.2 °C) with little precipitation (average 190 mm; period 1960 to 1990; ref. 48). Average daily air temperatures are typically above 0 °C from early to mid-June to September (data from Longyearbyen airport, ~13 km away from Grumant). Winter temperatures are much more variable than summer temperatures (48, 49). ROS (measured as amount of precipitation that fell at temperature above 1 °C from November to April) are relatively frequent stochastically
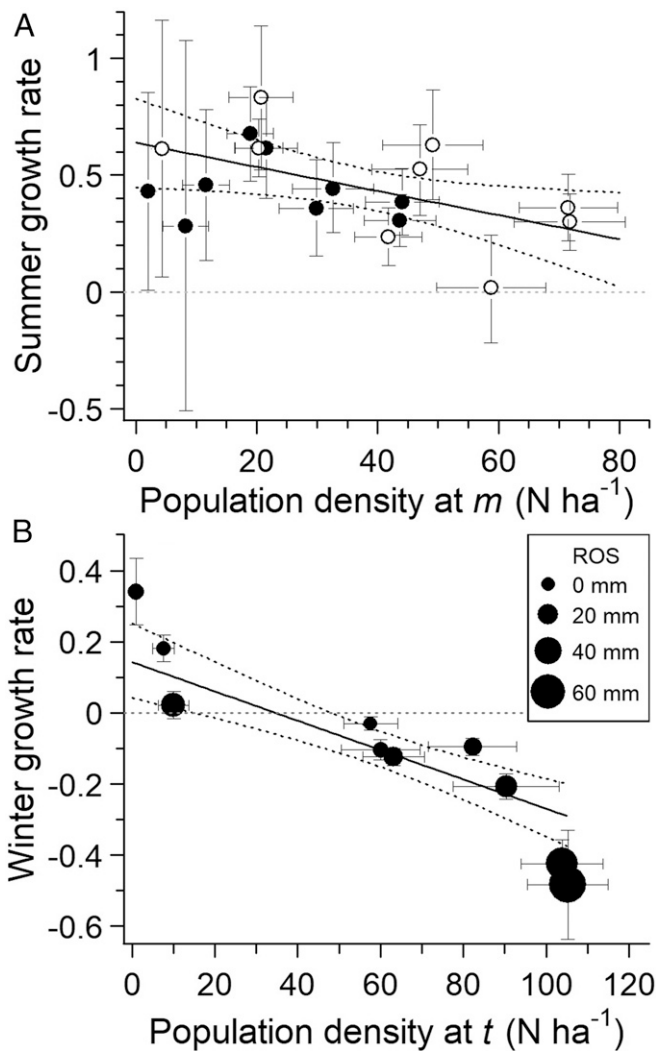
ECOLOGY

Fig. 3. Estimated monthly population growth rates (r) in summer in relation to population density in month m (*A*) and monthly winter population growth rate in relation with population density in year (t) measured in September (*B*) of East European voles. In *A*, filled points represent the early summer period (July to August) and open points the late summer period (August to September) each year. In *B*, the points represent average monthly growth over the period September to July and point size reflect the amount of ROS (millimeters) that fell during the winter. Error bars represent 95% CI and credibility intervals along the *x*- and *y*-axis, respectively. Parameter estimates for the regression lines (with 95% CI) are given in Table 1. Horizontal dotted gray line mark $r = 0$; no change in population size.

occurring weather events (30) and have been found to strongly influence the population dynamics of all year-round resident vertebrate populations in Svalbard (50).

The East European vole belongs to one of the most speciose and widespread genera (*Microtus*) of small mammals (51). Most *Microtus* species are graminivorous (grass-eating) and have multivoltine life histories (e.g., multiple generations per year). The East European vole was accidentally introduced to Svalbard in the first half of the 20th century (52). The voles have a highly restricted distribution on the archipelago, associated with seabird fertilized tundra vegetation dominated by graminoids (53).

There are no other small mammals present in Svalbard, which suggests no interspecific competition (54). The Arctic fox (*Vulpes lagopus*) is the only terrestrial predator present but acts as a generalist carnivore that mostly relies on large colonies of seabirds in the study area (55). Thus, the focal food web lacks the guild of specialist predators consisting of mustelids, owls, hawks, and jaegers that are almost omnipresent in the Arctic (12). East European voles reproduce quickly with females observed to be gravid as early

as 17 d old (56) and may live at high population densities (>100 individuals · ha^{-1}; ref. 54). Many *Microtus* populations have been studied extensively on the European continent where they typically exhibit 3- to 5-y multiannual cycles (11, 13–15).

Live Trapping. East European voles were live trapped during the years 1990 to 2007. Here, we analyzed two datasets. The main dataset used for analysis of seasonal density dependence and demography was obtained from one of the largest and lushest vole habitat patches in Svalbard, hereafter termed Core area (Fig. 1). From 1990 to 1996, we used a trapping grid of 93 Ugglan Special multiple-capture traps encompassing 4.5 ha of the Core area, while from 2002 to 2006, the grid was made of 74 traps and encompassed 2.8 ha. Traps were separated by ∼20 m and placed by burrow entrances wherever possible. Trapping of the Core area followed the robust design of Pollock (57) and consisted of three primary periods (late June/early July [hereafter termed July] = P1; early August = P2; and early September = P3), each with 6 to 10 secondary periods, except in 1990, when primary periods spanned only the first half of the summer. The primary trapping periods consisted of traps being checked at 1300 and 1900 after baiting with oats and potatoes in the morning (0700; i.e., two secondary periods per day). Traps were deactivated during the last trapping period of the day. We used a second, more long-term dataset obtained from a linear habitat on a ridge and vegetated part of the ravine at the western edge of the Core area (hereafter termed Ridge; Fig. 1) for assessing the annual population dynamics. The Ridge area was monitored with 30 traps in August during 1991 to 2007, with the same number of secondary periods as for the Core area. Captured voles were marked by toe clipping, sexed, and weighed. The study was conducted according to the regulations for research in Svalbard during the study period.

Density Estimation. The densities of the vole population in the Core and Ridge areas were estimated by spatially explicit capture–recapture (SECR) models with the package *secr* in R (58–60). Briefly, these models have the advantage of estimating capture probabilities based on the distance separating the center of activities of an individual from a trap (60). By using a two-parameter half-normal detection function, we obtained more accurate estimates of the area effectively surveyed (61). For the Core area, we used one null SECR model per trapping period per year with the Huggins parameterization to estimate density (61). For the Ridge area, annual densities were obtained for the August trapping period only. Densities of male and female adults (body mass ≥25 g) and subadults (body mass <25 g; ref. 56) were derived from this general model. Because the movement of voles in Svalbard is restricted by habitat, we used a 20-m buffer around traps to build the state-space that is used to estimate effective sampling area. The Nelder–Mead algorithm was used for optimization of the likelihood in model fitting.

Annual Density-Dependent Structure and Temporal Variability. We used the annual early August SECR density estimates from the Ridge area to assess the long dynamics of the system. The presence of cyclic dynamics was assessed using autocorrelations at different time lags. We used the SD of the log10-transformed time series as a metric for the temporal variability (i.e., the amplitude) of the multiannual dynamics (s-index; ref. 62). The s-index has been used both to define cyclic dynamics (index values > 0.5; ref. 63) and to compare populations across environmental gradients (31, 36, 64).

Table 1. Parameter estimates for the best models for monthly population growth of Eastern European voles (Eqs. 1–5) over winter and in the summer period and estimates of the Bayesian R^2 for the models

Parameter	Winter		Summer	
	Mean	95% CI	Mean	95% CI
β_0	0.23	0.14, 0.33	0.64	0.44, 0.83
β_D	−0.0040	−0.0058, −0.0024	−0.0051	−0.0095, −0.0006
β_{ROS}	−0.0043	−0.0074, −0.0014	—	—
σ_r^2	0.005	0.001, 0.020	0.020	0.005, 0.058
Bayesian R^2	0.92	0.73, 0.98	0.40	0.02, 0.76

No ROS effect was included in the model for summer population growth, giving no estimate of β_{ROS}. β_0 = intercept; β_D = coefficient for density at time t; β_{ROS} = coefficient for effect of ROS; and σ_r^2 = process error variance.
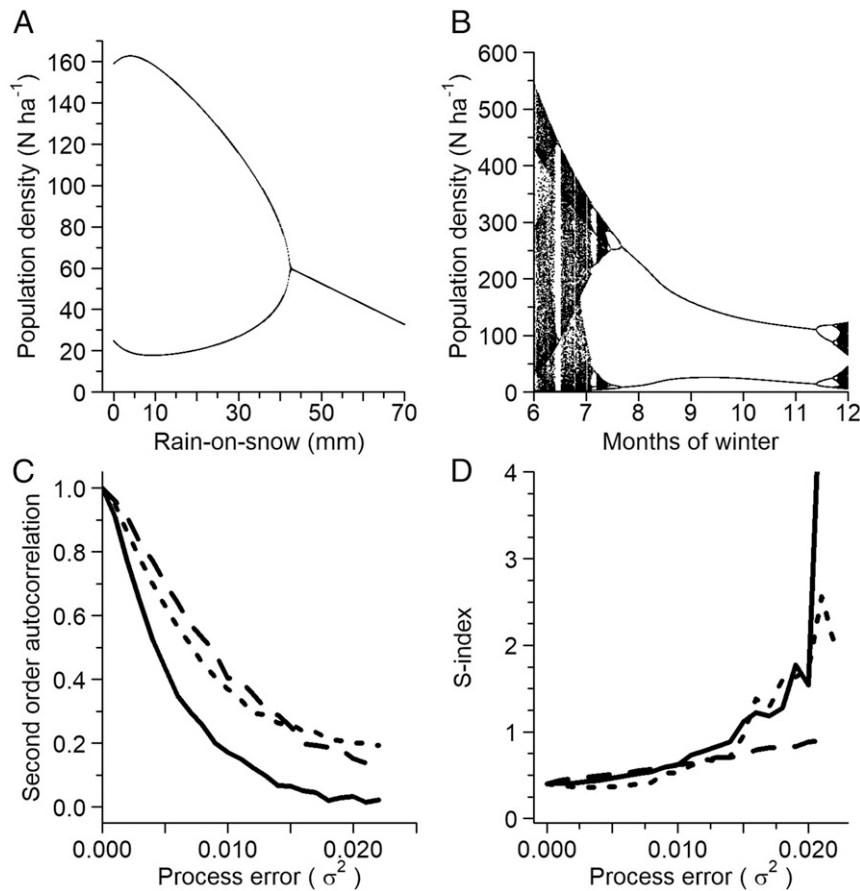
Fig. 4. Simulated population dynamics in the East European vole in Svalbard. (*A*) Bifurcation diagram for autumn densities for increasing fixed amounts of ROS every winter using the population model with no process error ($r_{w,t} = \beta_{w,0} + \beta_{w,X} * X_{w,t} + \beta_{w,ROS} * ROS_t$; parameter estimates in Table 1 but $\sigma_{i,r}^2$ set to zero). (*B*) Bifurcation diagram for the effect of changing the length of the winter season (Δt_w) on autumn densities in the baseline population model with zero ROS and process error (ROS = 0, $\sigma_r^2 = 0$). Estimates of the second order autocorrelation (*C*) and the amplitude of fluctuations (*s*-index) in autumn densities in the baseline population model for increasing values of process error variance (σ_r^2) and ROS = 0 (*D*). In *C* and *D*, the long, dashed line represents a model where process error only affects the summer population growth, the short, dashed line a model where process error only affects the winter population growth, and the solid line represents a model where process error affects equally winter and summer population growth. Estimates of process error variance in models without a ROS effects were $\overline{\sigma}_{w,r}^2 = 0.014$ and $\overline{\sigma}_{s,r}^2 = 0.020$ for winter and summer, respectively. Estimated second-order autocorrelation in the Ridge area in August was 0.02, while the *s*-index was 0.57.

Seasonal Density Dependence and Climate Effects on Population Growth. We used the following model to explore patterns of variation in population growth in summer and winter in the Core area:

$$X_{t+1} = X_t * e^{r_t * \Delta t}, \qquad [1]$$

where X_t is the true population density at time t, r_t is the population growth rate from t to $t+1$, and Δt is the time period from t to $t+1$ (in months). Furthermore, we modeled r_t as a linear function of X_t, weather variability measured by annual observations of ROS (in millimeters) in winter (ROS$_t$), and residual stochastic variation in r (process error, ε_t).

$$+r_t = \beta_0 + \beta_X * X_t + \beta_{ROS} * ROS_t + \varepsilon_t, \qquad [2]$$

where we assume that the process error $\varepsilon_t \sim N(0, \sigma_r^2)$ and β_0, β_X, β_{ROS}, and σ_r^2 are parameters estimated by the data. Measurement error was included in the model assuming a log normal distribution for the densities estimated using the SECR model, D_t, giving,

$$D_t \sim \text{lnorm}\left(\log_e(X_t), \sigma_{D,t}^2\right). \qquad [3]$$

The log normal measurement error SDs, $\sigma_{D,t}$, were calculated from the estimates of the SE of D_t (SE(D_t)) obtained in the SECR analysis:

$$\sigma_{D,t} = \log_e\left((\text{SE}(D_t)/D_t)^2 + 1\right). \qquad [4]$$

The model (Eqs. **1**–**3**) was fitted in JAGS version 4.2.0 (65). Point estimates of r_t and associated 95% credibility intervals presented in the figures were obtained by fitting a model for r_t (Eq. **2**) with time fitted as a factor (i.e., $r_t = \beta_t$). In addition to parameter estimates and associated 95% credibility intervals, we report estimates of Bayesian R^2 for the models (66). The Bayesian R^2 was calculated as the mean of $R_i^2 = \text{var}(\text{fit}_i)/(\text{var}(\text{fit}_i) + \text{var}(\text{residuals}_i))$, where i is the index of draws in Markov Chains Monte-Carlo sampling, $\text{var}(\text{fit}_i) = \text{var}(\beta_{0,i} + \beta_{X,i}*X_t + \beta_{ROS,i} * ROS_t)$, and $\text{var}(\text{residuals}_i) = \sigma_{r,i}^2$.

Analyses of population growth were done separately for the ~2.5-mo summer period (June/July to September) and for the ~9.5-mo winter period (September to June/July) as we expected the population dynamics to differ substantially in these two seasons. In the winter, we expected the amount of ROS to affect population growth (51, 67).

Summer population growth could be estimated from the change in densities from June/July (t) to August ($t + 1$) and from August ($t + 1$) to September ($t + 2$). Differences between these periods were investigated by fitting period as a factor in the model for population growth (Eq. **2**). Population growth rates were not estimated for the summer of 1996, when there were no voles captured in the study area, and 2002, when there were no voles captured in the first and second primary trapping periods and an estimate of one vole per hectare (three voles caught) in the third primary period. The very low density estimates in September 2002 and the absence of voles in 1996 implied adoption of methodological adjustments that are detailed in the *SI Appendix* to allow growth rate estimates over the associated winters.

The timing of the primary trapping periods differed somewhat in 1990 to 1991 from subsequent years. In 1990, all the trapping was early in the season and the time period from primary period 1 to primary period 3 was only 0.7 mo. We therefore only used data from primary period 1 and 3 to estimate

Fauteux et al.
Climate variability and density-dependent population dynamics: Lessons from a simple
High Arctic ecosystem

PNAS | 5 of 7
https://doi.org/10.1073/pnas.2106635118

population growth to get a time period that was more similar to the other years ($\Delta t = 1.2$ to 1.7 mo). In 1991, it was only 2 wk between primary period 1 and 2 and we used only estimates from primary period 2 and 3 in analyses.

Model Simulations of Multiannual Population Dynamics. We simulated the annual population dynamics linking summer and winter population growth using

$$X_{a,t} = X_{s,t} * e^{r_{s,t} * \Delta t_s} \text{ and} \tag{5}$$

$$X_{s,t+1} = X_{a,t} * e^{r_{w,t} * \Delta t_w}, \tag{6}$$

where $X_{s,t}$ and $X_{a,t}$ is population density in the spring and autumn in year (t), respectively, $r_{s,t}$ and $r_{w,t}$ are population growth rates (month^{-1}) in summer and winter, respectively, and Δt_s and Δt_w are the time periods of the summer and winter seasons, respectively ($\Delta t_s + \Delta t_w = 12$).

Using Eq. 2, $r_{j,t}$ were modeled with parameters estimated from the data (Table 1). Our baseline deterministic model included only density dependence

($r_{j,t} = \beta_{j,0} + \beta_{j,X} * X_{j,t}$) and assumed 3 mo of summer and 9 mo of winter. The sensitivity of population dynamics to changes in parameter values were evaluated using bifurcation diagrams and analyses of autocorrelation.

1. T. Royama, *Analytical Population Dynamics* (Springer, 1992).
2. P. Turchin, *Complex Population Dynamics* (Princeton University Press, Princeton, NJ, 2003).
3. R. M. May, *Stability and Complexity in Model Ecosystems* (Printeton University Press, Princeton, NJ, 2001).
4. N. C. Stenseth, Population cycles in voles and lemmings: Density dependence and phase dependence in a stochastic world. *Oikos* **87**, 427–461 (1999).
5. O. N. Bjørnstad, B. T. Grenfell, Noisy clockwork: Time series analysis of population fluctuations in animals. *Science* **293**, 638–643 (2001).
6. C. J. Krebs, *Population Fluctuations in Rodents* (The University of Chicago Press, Chicago, 2013).
7. C. S. Elton, *Voles, Mice and Lemmings. Problems in Population Dynamics* (Clarendon press, Oxford, 1942).
8. J. P. Finnerty, *The Population Ecology of Cycles in Small Mammals* (Yale University Press, New Haven, 1981).
9. N. C. Stenseth, R. A. Ims, *The Biology of Lemmings* (Academic Press, London, 1993).
10. F. Barraquand et al., Moving forward in circles: Challenges and opportunities in modelling population cycles. *Ecol. Lett.* **20**, 1074–1092 (2017).
11. F. Barraquand, A. Pinot, N. G. Yoccoz, V. Bretagnolle, Overcompensation and phase effects in a cyclic common vole population: Between first and second-order cycles. *J. Anim. Ecol.* **83**, 1367–1378 (2014).
12. R. A. Ims, E. Fuglei, Trophic interaction cycles in tundra ecosystems and the impact of climate change. *Bioscience* **55**, 311–322 (2005).
13. E. Korpimaki et al., Vole cycles and predation in temperate and boreal zones of Europe. *J. Anim. Ecol.* **74**, 1150–1159 (2005).
14. X. Lambin, V. Bretagnolle, N. G. Yoccoz, Vole population cycles in northern and southern Europe: Is there a need for different explanations for single pattern? *J. Anim. Ecol.* **75**, 340–349 (2006).
15. T. Cornulier et al., Europe-wide dampening of population cycles in keystone herbivores. *Science* **340**, 63–66 (2013).
16. N. C. Stenseth et al., Seasonality, density dependence, and population cycles in Hokkaido voles. *Proc. Natl. Acad. Sci. U.S.A.* **100**, 11478–11483 (2003).
17. T. F. Hansen, N. C. Stenseth, H. Henttonen, Multiannual vole cycles and population regulation during long winters: An analysis of seasonal density dependence. *Am. Nat.* **154**, 129–139 (1999).
18. K. Korpela et al., Nonlinear effects of climate on boreal rodent dynamics: Mild winters do not negate high-amplitude cycles. *Glob. Change Biol.* **19**, 697–710 (2013).
19. O. Gilg, B. Sittler, I. Hanski, Climate change and cyclic predator–prey population dynamics in the high Arctic. *Glob. Change Biol.* **15**, 2634–2652 (2009).
20. R. A. Ims, J. A. Henden, S. T. Killengreen, Collapsing population cycles. *Trends Ecol. Evol.* **23**, 79–86 (2008).
21. J. H. Myers, Population cycles: Generalities, exceptions and remaining mysteries. *Proc. Biol. Sci.* **285**, 20172841 (2018).
22. T. F. Hansen, N. C. Stenseth, H. Henttonen, J. Tast, Interspecific and intraspecific competition as causes of direct and delayed density dependence in a fluctuating vole population. *Proc. Natl. Acad. Sci. U.S.A.* **96**, 986–991 (1999).
23. R. S. Ostfeld, C. D. Canham, S. R. Pugh, Intrinsic density-dependent regulation of vole populations. *Nature* **366**, 259–261 (1993).
24. R. A. Ims, H. P. Andreassen, Spatial synchronization of vole population dynamics by predatory birds. *Nature* **408**, 194–196 (2000).
25. I. M. Graham, X. Lambin, The impact of weasel predation on cyclic field-vole survival: The specialist predator hypothesis contradicted. *J. Anim. Ecol.* **71**, 946–956 (2002).
26. O. Huitu, M. Koivula, E. Korpimaki, T. Klemola, K. Norrdahl, Winter food supply limits growth of northern vole populations in the absence of predation. *Ecology* **84**, 2108–2118 (2003).
27. D. Fauteux, G. Gauthier, D. Berteaux, Top-down limitation of lemmings revealed by experimental reduction of predators. *Ecology* **97**, 3231–3241 (2016).
28. B. T. Grenfell et al., Noise and determinism in synchronized sheep dynamics. *Nature* **394**, 674–677 (1998).
29. T. Coulson et al., Age, sex, density, winter weather, and population crashes in Soay sheep. *Science* **292**, 1528–1531 (2001).
30. B. B. Hansen et al., More frequent extreme climate events stabilize reindeer population dynamics. *Nat. Commun.* **10**, 1616 (2019).
31. D. Ehrich et al., Documenting lemming population change in the Arctic: Can we detect trends? *Ambio* **49**, 786–800 (2020).
32. L. Oksanen, Exploitation ecosystems in seasonal environments. *Oikos* **57**, 14–24 (1990).
33. P. Turchin, G. O. Batzli, Availability of food and the population dynamics of arvicoline rodents. *Ecology* **82**, 1521–1534 (2001).
34. M. Kot, W. M. Schaffer, The effects of seasonality on discrete models of population growth. *Theor. Popul. Biol.* **26**, 340–360 (1984).
35. E. R. White, A. Hastings, Seasonality in ecology: Progress and prospects in theory. *Ecol. Complex.* **44**, 100867 (2020).
36. L. Hansson, H. Henttonen, Rodent dynamics as community processes. *Trends Ecol. Evol.* **3**, 195–200 (1988).
37. O. N. Bjørnstad, W. Falck, N. C. Stenseth, A geographic gradient in small rodent density fluctuations: A statistical modelling approach. *Proc. Biol. Sci.* **262**, 127–133 (1995).
38. G. Gauthier, D. Berteaux, C. J. Krebs, D. Reid, Arctic lemmings are not simply food limited - a comment on Oksanen et al. *Evol. Ecol. Res.* **11**, 483–484 (2009).
39. P. Turchin, L. Oksanen, P. Ekerholm, T. Oksanen, H. Henttonen, Are lemmings prey or predators? *Nature* **405**, 562–565 (2000).
40. T. Klemola, M. Koivula, E. Korpimäki, K. Norrdahl, Experimental tests of predation and food hypotheses for population cycles of voles. *Proc. Biol. Sci.* **267**, 351–356 (2000).
41. R. Boonstra, C. J. Krebs, N. C. Stenseth, Population cycles in small mammals: The problem of explaining the low phase. *Ecology* **79**, 1479–1488 (1998).
42. O. Gilg, I. Hanski, B. Sittler, Cyclic dynamics in a simple vertebrate predator-prey community. *Science* **302**, 866–868 (2003).
43. I. Hanski, P. Turchin, E. Korpimäki, H. Henttonen, Population oscillations of boreal rodents: Regulation by mustelid predators leads to chaos. *Nature* **364**, 232–235 (1993).
44. J. Aars, R. A. Ims, Intrinsic and climatic determinants of population demography: The winter dynamics of tundra voles. *Ecology* **83**, 3449–3456 (2002).
45. F. Domine et al., Snow physical properties may be a significant determinant of lemming population dynamics in the high Arctic. *Arct. Sci.* **4**, 813–826 (2018).
46. L. Korslund, H. Steen, Small rodent winter survival: Snow conditions limit access to food resources. *J. Anim. Ecol.* **75**, 156–166 (2006).
47. K. L. Kausrud et al., Linking climate change to lemming cycles. *Nature* **456**, 93–97 (2008).
48. E. J. Førland, I. Hanssen-Bauer, P. Ø. Nordli, *Climate Statistics and Longterm Series of Temperature and Precipitation at Svalbard and Jan Mayen* (Norwegian Meteorological Institute, Oslo, 1997).
49. N. G. Yoccoz, R. A. Ims, Demography of small mammals in cold regions: The importance of environmental variability. *Ecol. Bull.* **47**, 137–144 (1999).
50. B. B. Hansen et al., Climate events synchronize the dynamics of a resident vertebrate community in the high Arctic. *Science* **339**, 313–315 (2013).
51. R. H. Tamarin, *Biology of New World Microtus* (American Society of Mammalogists, United-States, 1985).
52. K. Fredga, M. Jaarola, R. Anker Ims, H. Steen, N. G. Yoccoz, The 'common vole' in Svalbard identified as *Microtus epiroticus* by chromosome analysis. *Polar Res.* **8**, 283–290 (1990).
53. A. Elvebakk, A survey of plant associations and alliances from Svalbard. *J. Veg. Sci.* **5**, 791–802 (1994).
54. E. Koivisto, O. Huitu, E. Korpimaki, Smaller *Microtus* vole species competitively superior in the absence of predators. *Oikos* **116**, 156–162 (2007).
55. K. Frafjord, Predation on an introduced vole *Microtus rossiaemeridionalis* by arctic fox *Alopex lagopus* on Svalbard. *Wildl. Biol.* **8**, 41–47 (2002).
56. N. G. Yoccoz, R. A. Ims, H. Steen, Growth and reproduction in island and mainland populations of the vole *Microtus epiroticus*. *Can. J. Zool.* **71**, 2518–2527 (1993).
57. K. H. Pollock, A capture-recapture design robust to unequal probability of capture. *J. Wildl. Manage.* **46**, 752–757 (1982).

6 of 7 | PNAS
https://doi.org/10.1073/pnas.2106635118

Fauteux et al.
Climate variability and density-dependent population dynamics: Lessons from a simple High Arctic ecosystem

58. M. G. Efford, secr: Spatially explicit capture-recapture models. R Package Version 4.3.3. http://CRAN.R-project.org/package=secr. Accessed 15 January 2021.

59. R Core Team, *R: A Language and Environment for Statistical Computing* (R Foundation for Statistical Computing, Vienna, Austria, 2016).

60. D. L. Borchers, M. G. Efford, Spatially explicit maximum likelihood methods for capture-recapture studies. *Biometrics* **64**, 377–385 (2008).

61. C. J. Krebs *et al*., Density estimation for small mammals from livetrapping grids: Rodents in northern Canada. *J. Mammal.* **92**, 974–981 (2011).

62. N. C. Stenseth, E. Framstad, Reproductive effort and optimal reproductive rates in small rodents. *Oikos* **34**, 23–34 (1980).

63. H. Henttonen, A. D. McGuire, L. Hansson, Comparisons of amplitudes and frequencies (spectral analyses) of density variations in long-term data sets of *Clethrionomys* species. *Ann. Zool. Fenn.* **22**, 221–227 (1985).

64. L. Hansson, H. Henttonen, Gradients in density variations of small rodents: The importance of latitude and snow cover. *Oecologia* **67**, 394–402 (1985).

65. M. Plummer, "JAGS: A program for analysis of Bayesian graphical models using Gibbs sampling" in *Proceedings of the 3rd International Workshop on Distributed Statistical Computing* (Vienna, Austria, 2003).

66. A. Gelman, B. Goodrich, J. Gabry, A. Vehtari, Rsquared for Bayesian regression models. *Am. Stat.* **73**, 307–309 (2019).

67. A. Stien *et al*., Congruent responses to weather variability in high arctic herbivores. *Biol. Lett.* **8**, 1002–1005 (2012).

68. D. Fauteux, A. Stien, N. G. Yoccoz, E. Fuglei, R. A. Ims, Capture-recapture dataset of Svalbard voles (1990-2007) with trap locations and rain-on-snow measurements. *Dryad*. https://doi.org/10.5061/dryad.hhmgqnkhd. Deposited 25 August 2021.

ECOLOGY

Fauteux et al.
Climate variability and density-dependent population dynamics: Lessons from a simple High Arctic ecosystem